Synthesis, Characterization, Antimicrobial activity and Anti-cancerous efficacy (HeLa cell lines) by *Sargassum muticum* mediated synthesized silver nanoparticles

[1]Subramanian Poornima, [1*]Karuppiah Valivittan
Department of Biotechnology, St. Peter's University, Avadi, Chennai-600054

Abstract:
This work presents a simple method for the green synthesis of silver nanoparticles (AgNPs) using from brown algae *Sargassum muticum* present in the coast of Rameshwaram near mandapam camp. The AgNPS were prepared using silver nitrate solution and aqueous extract of algae at stirring for 30 min at 90°C. The formation of silver nanoparticles was monitored by measurements of UV–vis and FT-IR and characterized by size and zeta potential measurements using DLS and morphologically by TEM. The UV–vis absorption spectrum showed the surface plasmon peak at 369 nm, which is characteristic peak of silver nanoparticles. The functional biomolecules present in the algae interaction between the nanoparticles were identified by the Fourier transform infrared spectroscopy (FT-IR) analysis. XRD results shown that it is a Face Centered Cubic Lattice Structure (111), the hydrodynamic diameter of the AgNPs varied between 96.2 nm and Zeta potential of the silver nanoparticles was -7.8 mV. The AgNPs were tested for antimicrobial activity using (Gram-Positive and negative bacteria, fungal species) and Anti-cancer studies was done by using HeLa cell lines at *in-vitro* studies

Keywords: *Sargassum muticum, Silver nanoparticles, Anti-cancer activity, Antimicrobial activity*

Introduction

The field of nanotechnology is one among the foremost important and active areas of research in modern science. Nanotechnology deals with the formulation of experimental processes for the synthesis of nanoparticles with different sizes and shapes (Mahasneh 2013). The application of nanoparticles, usually ranging from 1 to 100 nm, is a developing and interesting area of nanotechnology (Dahl et al. 2007). Nanoparticles synthesized using metals have received extensive attention in recent years because of their remarkable properties and wide range of applications in catalysis (Paul et al. 2014), plasmonics (Khlebtsov and Dykman 2010), optoelectronics (Muruganandam et al. 2014), biological sensor (Venkatesan and Santhanalakshmi 2014), water treatment (Con and Loan 2011) and pharmaceutical applications (Ravichandran 2009). To date, metallic nanoparticles are mostly prepared from noble metals, i.e. silver (Vankar and Shukla 2012), gold (Dash et al. 2014), copper, zinc and titanium (Schabes-Retchkiman et al. 2006) as well from cadmium (Suresh 2014), iron (Behera et al. 2013) and alginate (Asadi 2014). Among the noble metals, silver (Ag) is the metal of choice in the field of biological system, living organisms and medicine (Parashar et al. 2009). It is generally recognized that silver nanoparticles may adhere to the cell wall and damage the cell wall permeability. The cellular DNA and protein are destroyed by interaction of nanoparticles with the phosphorus of DNA and sulphur containing amino acids of protein (Elumalai et al. 2010). Different types of methods are available for the synthesis of silver nanoparticles for example, reduction in solutions (Goia and Matijevic 1998), chemical and photochemical reactions in reverse micelles (Taleb et al. 1997), thermal decomposition of silver compounds (Esumi et al. 1990), radiation assisted (Shahriari et al. 2011), electrochemical (Li et al. 2008), sonochemical (Moghimi-Rad et al. 2011), microwave assisted (Pal et al. 2014) and recently via green chemistry approach (Gao et al. 2014).

Green synthesis of nanoparticles is an emerging branch of nanotechnology. The use of environmentally benign materials like plant extract (Supraja et al. 2015), bacteria (Seshadri et al. 2012), fungi (Muhsin and Hachim 2014) and marine algae (Supraja et al. 2016) for the synthesis of silver nanoparticles offers numerous benefits of eco-friendliness and compatibility for pharmaceutical and other biomedical applications as they do not use toxic chemicals for the synthesis protocol. Green synthesis are found to be superior over physical and chemical method as it is economically feasible, environmental friendly, scaled up for mass-scale production without any complexity.

The present study describes a single step, green, and rapid synthesis of silver nanoparticles (Ag-NPs) prepared by biological (green) techniques using *Sargassum muticum* (*S. muticum*). These green-synthesized nanoparticles were examined by ultraviolet-visible spectroscopy (UV–Vis), transmission electron microscopy (TEM), Dynamic Light Scattering (DLS), powder X-ray diffraction (XRD) and Fourier transform infrared (FT-IR) spectroscopy to determine their size and shape.

Methodology

Materials

Silver nitrate (>99% pure) was purchased from Sigma Aldrich, India. Potato dextrose broth, Potato dextrose agar, Nutrient broth, Nutrient agar plate, was supplied by Hi-media, India

Sample collection and preparation (*Sargassum muticum*)

The brown algae (*Sargassum muticum*) were collected from the rameshwaram sea coast area, Tamilnadu, India and were brought to the nanotechnology laboratory and washed with distilled water several times to remove the impurities. The clean algae were dried at room temperature in the shade for a week and powdered using a mortar and pestle

Preparation of *Sargassum muticum* (brown algae) extract

Dried powdered *Sargassum muticum* (5g) was mixed with 100ml distilled water then the solution was kept for continues heating at 80°C for 1hour at room temperature with frequent shaking. After that the extract were filtered by using Whatmann No1 filter paper. The extract was collected and stored at 4°C for further use.

Synthesis of silver nanoparticles from *Sargassum muticum*

10 ml of the aqueous extract of *Sargassum muticum* was added into 90ml of aqueous solution of 1mM Silver nitrate. The mixture was exposed to a range of controlled temperatures for 24h. Appearance of brown color in solution indicated the formation of AgNPs. The solution was then kept in dark for further analysis collected and stored at 4°C for further use.

Collection of microbes (Bacteria and fungi)

The microbes (Bacteria and fungi) samples were collected from Department of Biotechnology, Thiruvalluvar University, Vellore, Tamil Nadu, India. These samples were stored in an ice box and transported to the laboratory for microbiological characterization. Through serial dilution pour plate technique, fungal sp. was isolated using potato dextrose agar (PDA) medium, and Gram negative and Gram-positive bacteria were isolated from nutrient agar medium. Further, it is maintained in potato dextrose agar slants (fungi) and nutrient agar slants (bacteria) for onward analysis.

Antimicrobial activity

Antibacterial activity of *Sargassum muticum* produced AgNPs

The antibacterial activity of AgNPs was evaluated against the following pathogenic strains *E. coli*, *Pseudomonas Fluorescence*, *Staphylococcus aureus*, *Sphingobacterium thalpophilum*, *Legionella pneumonia*, *Actinomyces israelii*, *Enterobacter cloacae*, *Helicobacter pylori*, *Acinetobacter* and *Bacillus subtilis*. These cultures were grown on appropriate medium at 37°C for overnight incubation and maintained at 4°C in a refrigerator. Disc diffusion method disc of 5Mm was made for nutrient agar medium and each disc was dipped at different concentration (170, 100, 50ppm) efficiency of prepared AgNPs. The pure cultures of bacterial pathogens were sub-cultured on an appropriate medium. For comparison, plate of the same diameter with 5Mm Cefmetazole (30mcg) was used. After incubation at 37°C for 24h the zones of bacterial inhibition were measured. The assays were performed triplicate.

Antifungal activity of *Sargassum muticum* produced AgNPs

The antifungal activity of AgNPs was evaluated against the following pathogenic strains *Aspergillus niger*, *Aspergillus flavus*, *Schelorosium rolfsii*, *Rhizopus oligosporus*, *Aspergillus acidus*, *Athelia rolfsii*, *Aspergillus fumigates*, *Rhizopus oryzae*, *Tricoderma asperellum* and *Meyerozyma caribbica.* These cultures were grown on appropriate medium at 37°C for overnight incubation and maintained at 4°C in a refrigerator. Disc diffusion method disc of 5Mm was made on nutrient agar medium and each disc was dipped at different concentration (170, 100, 50ppm) efficiency of prepared AgNPs. The pure cultures of fungal pathogens were sub-cultured on an appropriate medium. Discs of 5 mm diameter were made on potato dextrose agar medium. Each strain was swabbed uniformly onto the individual plate. For comparison, plate of the same diameter with 5Mm itraconazole (30mcg) was used. After incubation at 37°C for 24h the zones of fungal inhibition were measured. The assays were performed triplicate.

Anti cancer activity of *Sargassusm muticum* produced AgNPs towards (HeLa) cell lines

Cell line

The human cervical cancer cell line (HeLa) was obtained from National Centre for Cell Science (NCCS), Pune and grown in Eagles Minimum Essential Medium containing 10% fetal bovine serum (FBS). The cells were maintained at 37^0C, 5% CO2, 95% air and 100% relative humidity. Maintenance cultures were passaged weekly, and the culture medium was changed twice a week.

Cell treatment procedure

The monolayer cells were detached with trypsin-ethylenediaminetetraacetic acid (EDTA) to make single cell suspension. Viable cells were counted by tryphan blue exclusion using a hemocytometer and diluted with medium containing 5% FBS to give final density of $1x10^5$ cells/ml. One hundred microlitres per well of cell suspension were seeded into 96-well plates at plating density of 10,000 cells/well and incubated to allow for cell attachment at 37^0C, 5% CO_2, 95% air and 100% relative humidity. After 24 h the cells were treated with serial concentrations of the test samples.

They were initially dispersed in phosphate buffered saline (PBS) and an aliquot of the sample solution was diluted to twice the desired final maximum test concentration with serum free medium. Additional four serial dilutions were made to provide a total of five sample concentrations. Aliquots of 100 µl of these different sample dilutions were added to the

appropriate wells already containing 100 µl of medium, resulting in the required final sample concentrations. Following sample addition, the plates were incubated for an additional 48 h at 37^0C, 5% CO_2, 95% air and 100% relative humidity. The medium containing without samples were served as control and triplicate was maintained for all concentrations.

MTT assay

3-[4,5-dimethylthiazol-2-yl]2,5-diphenyltetrazolium bromide (MTT) is a yellow water soluble tetrazolium salt. A mitochondrial enzyme in living cells, succinate-dehydrogenase, cleaves the tetrazolium ring, converting the MTT to an insoluble purple formazan. Therefore, the amount of formazan produced is directly proportional to the number of viable cells.

After 48 h of incubation, 15µl of MTT (5mg/ml) in phosphate buffered saline (PBS) was added to each well and incubated at 37^0C for 4h. The medium with MTT was then flicked off and the formed formazan crystals were solubilized in 100µl of DMSO and then measured the absorbance at 570 nm using micro plate reader. The percentage cell growth was then calculated with respect to control as follows

% Cell Growth = [A] Test / [A]control x 100

Characterization of Ag nanoparticles

UV – Visible spectrum for synthesized nanoparticles

The nanoparticles were monitored by UV–visible spectrum at various time intervals. The UV – Visible spectra of this solution was recorded in spectra 50 ANALYTIKJENA Spectrophotometer, from 250 to 400nm.

FT-IR Analysis for synthesized nanoparticles

The nanoparticles were harvested and characterized by FT-IR. The FT-IR spectrum was taken in the mid IR region of 400–4000 cm^{-1}. The spectrum was recorded using ATR (attenuated total reflectance) technique. The sample was directly placed in the KBr crystal and the spectrum was recorded in the transmittance mode.

X-ray Diffraction analysis for synthesized nanoparticles

The nanoparticles were harvested and characterized by XRD and TEM. The XRD pattern was recorded using computer controlled XRD-system, JEOL, and Model: JPX-8030 with CuK radiation (Ni filtered = 13418 A^o) at the range of 40kV, 20A. The 'peak search' and 'search match' program built in software (syn master 7935) was used to identify the peak table and ultimately for the identification of XRD peak.

Particle Size and Zeta potential analyzer for synthesized nanoparticles

The aqueous suspension of the synthesized nanoparticles was filtered through a 0.22 µm syringe driven filter unit and the size of the distributed nanoparticles were measured by using the principle of Dynamic Light Scattering (DLS) technique made in a Nanopartica (HORIBA, SZ-100) compact scattering spectrometer.

Transmission electron microscopy (TEM)

The surface morphology and size of the nanoparticles were studied by transmission electron microscopy (JEOL (JEM-1010)) with an accelerating voltage of 80 kV. A drop of aqueous AgNPs on the carbon-coated copper TEM grids was dried and kept under vacuum in desiccators before loading them onto a specimen holder. The particle size and surface morphology of nanoparticles were evaluated using ImageJ 1.45s software.

Results and discussion

In the present study, the brown algal *Sargassum muticum* used in the green synthesis of AgNPs forming complexes with the silver ions and thereby controlling the process of reduction is to stabilize and protect the particles from aggregation. Used a green protocol for the synthesis of silver nanoparticles with algal extract extracted from *Sargassum muticum*. In the present study, the seaweed *Sargassum muticum* was used because it is very commonly found in Rameshwaram a simple procedure to extract from the algae was used

UV-Visible spectral analysis (*Sargassum muticum*)

It is well- known that silver nanoparticles exhibit brown color, which arises due to excitation of surface Plasmon vibrations of the silver nanoparticles. After addition of 1mM silver nitrate solution to the aqueous extract Sargassum muticum **(Fig.1)**, the colour of the composition has been changed to dark brown colour. The maximum absorbance peak is observed at 369 nm for *Sargassum muticum* **(Fig. 2)**. The overall observations suggest that the bio reduction of (silver ions) Ag^+ to $Ag^{(0)}$ was confirmed by UV-Visible spectroscopy.

Fourier Transform Infrared Spectrophotometry analysis (*Sargassum muticum)*

FT-IR spectrum of the biosynthesized silver nanoparticles using *Sargassum muticum* **(Fig. 3)** shows the absorption peaks at 3358, 2885, 2820, 2104, 1636, 1394 and 582cm^{-1}. The peak at 3358 cm^{-1} reveals the presence of N-H stretching vibration, indicating the primary and secondary amines, 2885 and 2820cm^{-1} reveals the presence of C-H stretching vibration, indicating the presence of carboxylic/phenolic groups, 2104cm^{-1} reveals the presence of C-H stretching vibration, indicating the presence of alkanes, 1636cm^{-1} reveals indicating the presence of [N-H] C=O group

that is characteristic of proteins shifted from after the synthesis of AgNPs, 1394cm^{-1} reveals the presence of amide II and amide III of aromatic rings and 582cm^{-1} indicates C-Br stretching vibration of alkyl halides either may be poly phenols associated with synthesized silver nanoparticles which is segregated by *Sargassium muticum* extract.

X-Ray Diffraction analysis (*Sargassum muticum)*

The sample of AgNPs could be also characterized by X-Ray Diffraction analysis of dry powder. The diffraction intensities were recorded from 10°-80° at 2θ angles **(Fig.4)**. Four different and important characteristic peaks were observed at the 2θ of 38.6°, 45.8°, 64.8° and 78.6° that correspond to (111), (200), (311) and (222) planes, respectively. All the peaks in XRD pattern can be readily indexed to a face centered cubic structure of silver as per available literature (JCPDS, File No. 4-0785). The XRD pattern of these peaks indicates the AgNPs is crystalline in nature and some of the unassigned peaks were observed it may be due to the fewer bio-molecules of stabilizing agents are enzymes or proteins in the *Sargassum muticum* extract.

Dynamic light scattering analysis (*Sargassum muticum)*

The particle size distribution spectra for the silver nanoparticles were recorded as diameter (nm) verses frequency (%/nm) spectra with diameter (nm) on x-axis and frequency (%/nm) on y-axis. The zeta potential spectra for the silver nanoparticles were recorded zeta potential verses intensity spectra with zeta potential (mV) on x-axis and intensity (a.u) on y-axis. Dynamic light scattering technique has been used to measure hydrodynamic diameter of the hydrosol (particle suspension). *Sargassum muticum* AgNPs was found to be 96.2nm **(Fig. 5a)** the recorded value of zeta potential of the silver nanoparticles was -7.8mV **(Fig. 5b)** which resulted in the agglomerated state of the formed AgNPs.

Transmission Electron Microscopic analysis (*Sargassum muticum)*

The size and shape of bio-reductant nanoparticles from *Sargassum muticum* were characterized and shown by the TEM micrograph of silver nanoparticles **(Fig. 6)**. It is evident from the micrograph that individual silver nanoparticles as well as a number of aggregates are present and they are spherical in shape with an average particle size of 0.2µm-50 nm.

Antimicrobial activity of *Sargassum muticum aqueous* extract mediated silver nanoparticles

It is well- known that silver nanoparticles exhibit brown color, arising due to excitation of surface Plasmon vibrations in the silver nanoparticles. Silver nanoparticles obtained from *Sargassum muticum* shown have very strong inhibitory action against fungal sp, Gram-positive and Gram-negative bacteria. These isolates were collected from nanotechnology laboratory, Acharya N G Ranga Agricultural University, Tirupathi. Three concentrations of NPs (170, 100, 50ppm) were prepared and were applied against an array of bacterial species *viz., Escherichia coli, Staphylococcus aureus, Pseudomonas fluorescence, Sphingobacterium thalpophilum, Legionella pneumonia, Actinomyces israelii, Enterobacter cloacae, Helicobacter pylori, Acinetobacter* and *Bacillus subtilis*, fungal species *viz., Aspergillus niger, Aspergillus flavus, Sclerotium rolfsii, Rhizopus oligosporus, Aspergillus acidus, Athelia rolfsii, Aspergillus fumigates, Rhizopus oryzae, Tricoderma asperellum* and *Meyerozyma caribbica*. The higher concentration (170ppm) of AgNPs showed significant antimicrobial effect compared with other concentrations (100, 50ppm and antibiotic discs). Following the silver nanoparticles treatment, the cytoplasm membrane shrank and became separated from the cell wall. Cellular contents were then released from the cell wall, and the cell wall was degraded. These phenomena suggest possible antibacterial mechanisms by which silver ions inhibit bacterial growth, as well as cellular responses of both the gram-positive and gram-negative bacteria to the silver ion treatment. Although the mechanisms underlying the antibacterial actions of silver are still not fully understood, several previous reports **(**McDonnell and Russell. 1999; Pal et al. 2007; Sondi and Salopek-Sondi 2004) showed that the interaction between silver and the constituents of the bacterial membrane caused structural changes and damage to the membranes and intracellular metabolic activity which might be the cause or consequence of cell death, as demonstrated in this study. Moreover, *Sargassum muticum* AgNPs showed good antibacterial and antifungal activity **(Fig. 7a and 7b)**, **(Table. 1 and 2)**. The findings in this study may lead to the development of AgNPs-based new antimicrobial systems for medical applications.

Anti cancer activity of HeLa (Human Cervical cancer cell lines)

The cytotoxic effect of *Sargassum muticum* mediated synthesis of AgNPs was evaluated in vitro against Human cervical cancer cell lines (HeLa) cell lines at five different concentrations (12.5, 25, 50, 100 and 200µg/mL) by MTT assay and the results are depicted in **(Fig. 8 and 9)**. The in vitro screening of the synthesized AgNPs exhibited the percentage viability of HeLa cell lines decreased with increased concentration of AgNPs in a dose dependent manner. This study clearly indicated that the size and dose of AgNPs as well as cells used in the experiment play a crucial role in the cytotoxic effect of AgNPs. Similarly, the cytotoxic effect exhibited by different types of silver nanoparticles on HeLa cell line and the variance due to concentration of nanoparticles **(Table. 3)**

The change in color of the solution was observed (from colorless to dark brown color) after keeping the solution at 50°C for 25 min. In the case of silver, the reduction started within 5 min after the addition and completed in 30 min. The possible explanation of difference in the reduction time could be due to the difference in their reduction potential for both the metal ions. Metal nanoparticles such as silver have free electrons, which give rise to SPR absorption band.

From the FT-IR spectra of *Sargassum muticum* extract samples, change in wave number of the functional groups was observed due to the reduction and stabilization of metal group, the nanoparticles are bound to the functional organic

groups (carboxyl and amine) and these functional groups may act as template, reducing and capping agents of silver nanoparticles.

This clearly indicates that the silver nanoparticles formed by the reduction of Ag+ ions by the algal extracts are crystalline in nature. The relatively higher intensity of (111) plane in FCC crystal structure supports the enhanced antimicrobial activity of the prepared AgNPs. The crystalline size was calculated from the width of the peaks present in the XRD pattern, assuming that they are free from non-uniform strains, using the Debye–Scherrer formula

$D = 0.94\ \lambda/\beta\cos\theta$

Where D is the average crystalline domain size perpendicular to the reflecting planes, λ (1.5406×10^{-10}) is the X-ray wavelength used, β is the full width at half maximum (FWHM) and θ is the diffraction angle. The calculated crystalline size of the AgNPs was 50 nm and further it also confirms that the synthesized nano powder was free of impurities as it does not contain any characteristics XRD peaks other than AgNPs.

Dynamic light scattering technique has been used to measure hydrodynamic diameter of the hydrosol (particle suspension). Particle size determination of the formulated AgNPs was shown under different categories like size distribution by volume and intensity. The size distribution by volume gives a bell shaped pattern which indicates the wide range size distribution of nanoparticles in the sample formulation. The volume % of the samples was found to be in the range of $0.1–1 \times 10^6$ (AgNPs). The formed AgNPs are well distributed with respect to volume and intensity, an indication of the formation of well built AgNPs and their mono and poly disparity, respectively.

The recorded value of zeta potential of the silver nanoparticles which resulted in the agglomerated state of the formed AgNPs. If the hydrosol has a large negative or positive zeta potential (C30 mV), then the particles tend to repel with each other and show no tendency to agglomerate resulted in polydispersed particles. The formed AgNPs appears slightly aggregated due to the absence of strong surface protecting ligands and found to be spherical in shape. The particles were crystalline in nature as revealed by the XRD analysis.

The experimental results in the present study indicated that the silver nanoparticles has anticancer activity through induction of apoptosis in HeLa cancer cell line, suggesting that AgNPs might be a potential alternative therapeutic agent for human cancer. The morphological changes of HeLa cancer cells were observed in this study when they were treated with AgNPs with different concentrations. They suggested that generation of reactive oxygen species plays key role in the induction of apoptosis in all HeLa cancer cells.

It is well known that Ag ions and Ag-based compounds have strong biological activities, However, Ag ions or salts has only limited usefulness for several reasons, including the interfering effects of salts and the continuous release of enough concentration of Ag ion from the metal form. In contrast, these kinds of limitations can be overcome by the use of AgNPs. However, to use AgNPs in various fields, it is essential to prepare the AgNPs with a cost effective method. In this study we were able to prepare AgNPs eco-friendly and cost effectively by using the aqueous extracts from different Sea weeds (*Sargassum muticum)*, and these AgNPs were homogeneous. Owing to their small size, AgNPs impair the sulfur and phosphorus containing essential macromolecules such as proteins and DNA, Thus, action of AgNPs appears to be a consequence of adherence to and penetration inside the cell of the target cells. In this study, anti-cancer activity of AgNPs on HeLa was investigated. Cells were observed to exhibit different responses after treatment with AgNPs.

Conclusion

In the present study, we demonstrated the stable green synthesis of an AgNP solution with brown algae *Sargassum muticum* reducing and stabilizing agent. The resulted particles exhibited favorable characteristics, including the spherical shape, hydrodynamic diameter between 96.2 nm and positive zeta potential -7.8mv. The synthesized AgNPs showed very good antimicrobial activity with greater efficacy against bacteria than fungi, probably due to the shape and the size of AgNP, Anti-cancer efficacy of HeLa cell lines showed very less cytotoxicity. This kind of study may also serve as a model for the future preparation of nano-medicines, Agricultural spraying and Industrial Applications.

References

[1] Mahasneh AM (2013) Bionanotechnology: the novel nanoparticles based approach for disease therapy. Jordan J Biol Sci 6:246–251

[2] Dahl JA, Maddux BL, Hutchison JE (2007) Toward greener nanosynthesis. Chem Rev 107:2228–2269

[3] Paul K, Bag BG, Samanta K (2014) Green coconut (Cocos nucifera Linn.) shell extract mediated size controlled green synthesis of polyshaped gold nanoparticles and its application in catalysis. Appl Nanosci 4:769–775

[4] Khlebtsov NG, Dykman LA (2010) Optical properties and biomedical applications of plasmonic nanoparticles. J Quant Spectrosc Radiat Transfer 111:1–35

[5] Muruganandam S, Anbalagan G, Murugadoss G (2014) Optical, electrochemical and thermal properties of Co2?-doped CdS nanoparticles using polyvinylpyrrolidone. Appl Nanosci. doi:10. 1007/s13204-014-0313-6

[6] Venkatesan P, Santhanalakshmi J (2014) Synthesis, characterization and catalytic activity of gold and silver nanoparticles in the biosensor application. J Exp Nanosci 9:293–298
[7] Con TH, Loan DK (2011) Preparation of silver nano-particles and use as a material for water sterilization. Environ Asia 4:62–66
[8] Ravichandran R (2009) Nanoparticles in drug delivery: potential green nanobiomedicine applications. Int J Nanotechnol Biomed 1:108–130
[9] Vankar PS, Shukla D (2012) Biosynthesis of silver nanoparticles using lemon leaves extract and its application for antimicrobial finish on fabric. Appl Nanosci 2:163–168
[10] Dash SS, Majumdar R, Sikder AK, Bag BG, Patra BK (2014) Saraca indica bark extract mediated green synthesis of polyshaped gold nanoparticles and its application in catalytic reduction. Appl Nanosci 4:485–490
[11] Schabes-Retchkiman PS, Canizal G, Herrera-Becerra R, Zorrilla C, Liu HB, Ascencio JA (2006) Biosynthesis and characterization of Ti/Ni bimetallic nanoparticles. Opt Mater 29:95–99
[12] Suresh S (2014) Studies on the dielectric properties of CdS nanoparticles. Appl Nanosci 4:325–329
[13] Behera T, Swain P, Rangacharulu PV, Samanta M (2013) Nano-Fe as feed additive improves the hematological and immunological parameters of fish, Labeo rohita H. Appl Nanosci 4:687–694
[14] Asadi A (2014) Streptomycin-loaded PLGA-alginate nanoparticles: preparation, characterization, and assessment. Appl Nanosci 4:455–460
[15] Parashar V, Parashar R, Sharma B, Pandey AC (2009) Parthenium leaf extract mediated synthesis of silver nanoparticles: a novel approach towards weed utilization. Dig J Nanomater Bios 4:45–50
[16] Elumalai EK, Prasad TNVKV, Kambala V, Nagajyothi PC, David E (2010) Green synthesis of silver nanoparticle using Euphorbia hirta L. and their antifungal activities. Archives Appl Sci Res 2:76–81
[17] Goia D, Matijevic E (1998) Preparation of monodispersed metal particles. New J Chem 22:1203–1215
[18] Taleb A, Petit C, Pileni MP (1997) Synthesis of highly monodisperse silver nanoparticles from AOT reverse micelles: a way to 2D and 3D self-organization. Chem Mater 9:950–959
[19] Esumi K, Tano T, Torigoe K, Meguro K (1990) Preparation and characterization of bimetallic palladium- copper colloids by thermal decomposition of their acetate compounds in organic solvents. Chem Mater 2:564–567
[20] Shahriari E, Yunus WMM, Talib ZA, Saion E (2011) Thermalinduced non-linearity of Ag nano-fluid prepared using cradiation method. Sains Malaysiana 40:13–15
[21] Li N, Bai X, Zhang S, Gao YA, Zheng L, Zhang J, Ma H (2008) Synthesis of silver nanoparticles in ionic liquid by a simple effective electrochemical method. J Dispers Sci Technol 29:1059–1061
[22] Moghimi-Rad J, Isfahani TD, Hadi I, Ghalamdaran S, Sabbaghzadeh J, Sharif M (2011) Shape-controlled synthesis of silver particles by surfactant self-assembly under ultrasound radiation. Appl Nanosci 1:27–35
[23] Pal J, Deb MK, Deshmukh DK (2014) Microwave-assisted synthesis of silver nanoparticles using benzo-18-crown-6 as reducing and stabilizing agent. Appl Nanosci 4:507–510
[24] Gao Y, Huang Q, Su Q, Liu R (2014) Green synthesis of silver nanoparticles at room temperature using kiwifruit juice. Spectrosc Lett 47:790–795
[25] Supraja N, Prasad TNVKV, Giridhar Krishna T, David E (2015) Synthesis, Characterization and Evaluation of the antimicrobial efficacy of *Boswellia ovalifoliolata* stem bark extract mediated zinc oxide nanoparticles. Applied nanoscience DOI 10.1007/s13204-015-0472-0
[26] Seshadri S, Prakash A, Kowshik M (2012) Biosynthesis of silver nanoparticles by marine bacterium, Idiomarina sp. PR58-8. Bull Mater Sci 35:1201–1205
[27] Muhsin TM, Hachim AK (2014) Mycosynthesis and characterization of silver nanoparticles and their activity against some human pathogenic bacteria. World J Microb Biot 30:2081–2090
[28] Supraja N, Prasad TNVKV, Soundariya M, Babujanarthanam R (2016) Synthesis, characterization and dose dependent antimicrobial and anticancerous activity of phycogenic silver nanoparticles against human hepatic carcinoma (HepG2) cell line. AIMS Bioengineering, 3 (4): 425-440.

Fig 1: *Sargassum muticum*

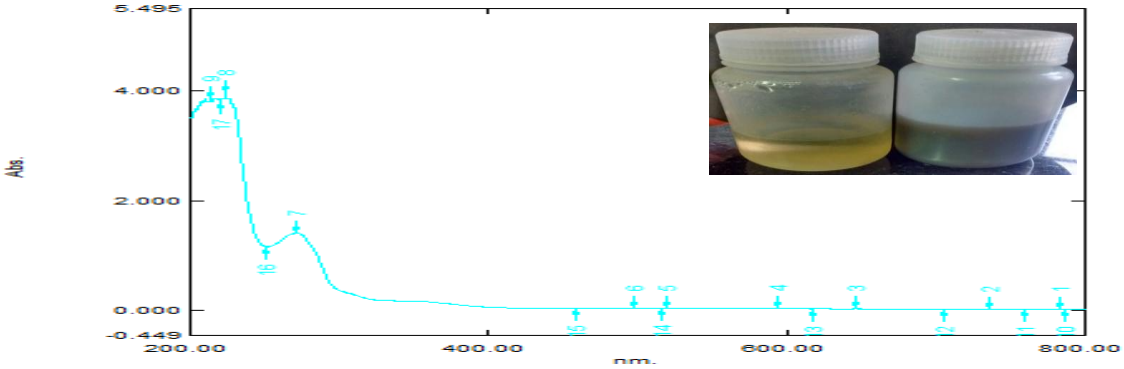

Fig 2: UV-visible spectroscopy showing *Sargassum muticum* mediated synthesized silver nanoparticles

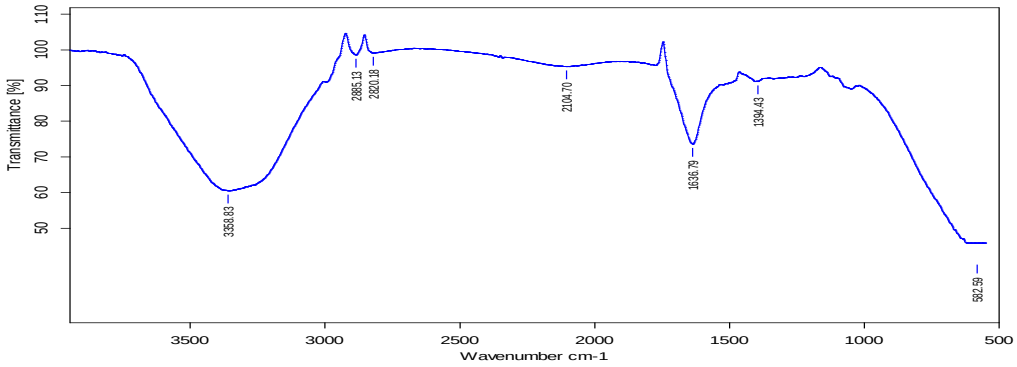

Fig 3: FT-IR spectroscopy showing *Sargassum muticum* mediated synthesized silver nanoparticles

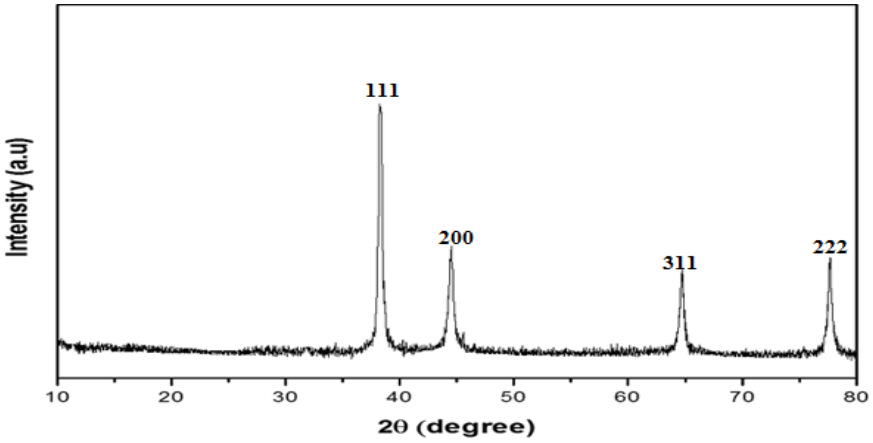

Fig 4: XRD analysis showing *Sargassum muticum* mediated synthesized silver nanoparticle

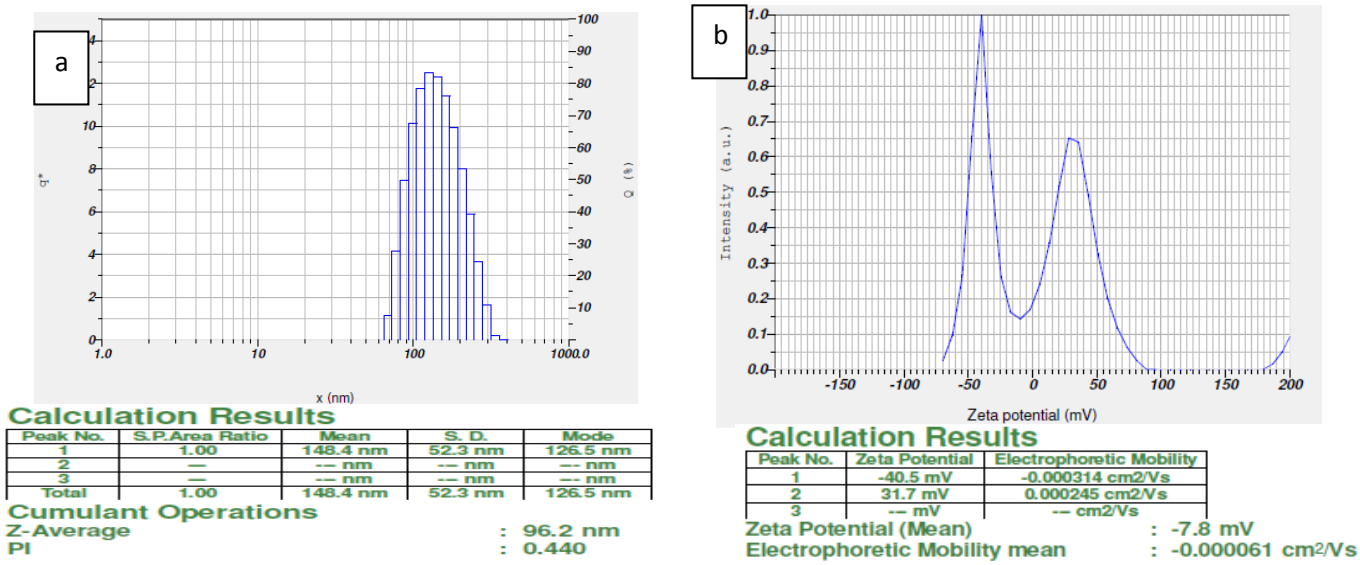

Fig 5: DLS analysis showing a) Particle size b) Zeta potential *Sargassum muticum* mediated synthesized silver nanoparticles

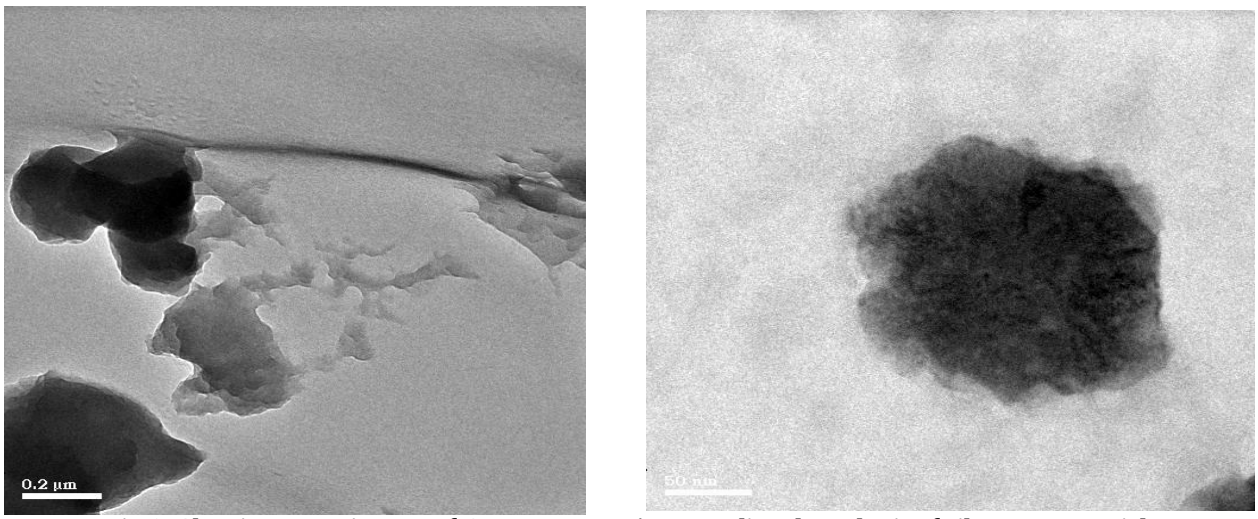

Fig 6: Showing TEM images of *Sargassum muticum* mediated synthesis of silver nanoparticles

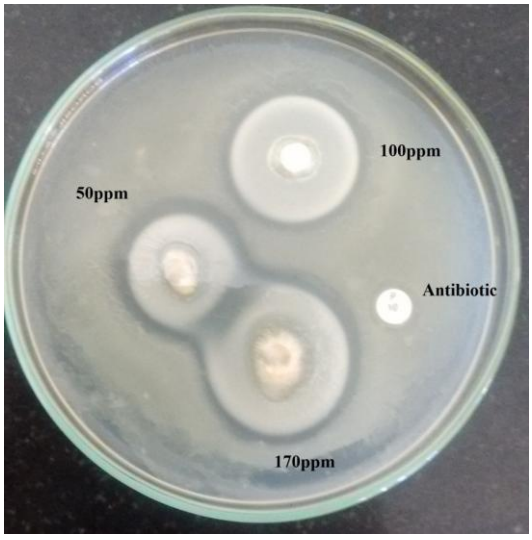

E. coli

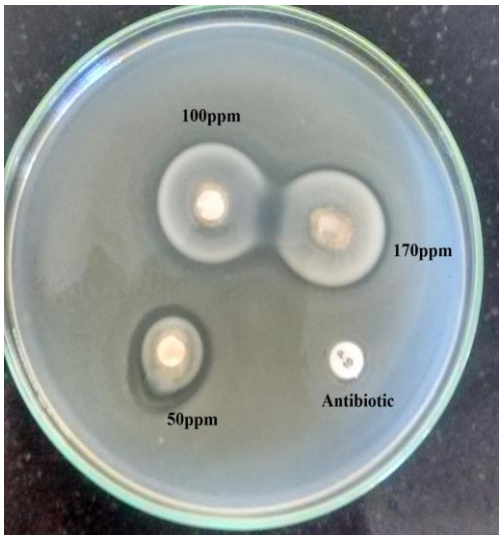

Pseudomonas Fluorescence

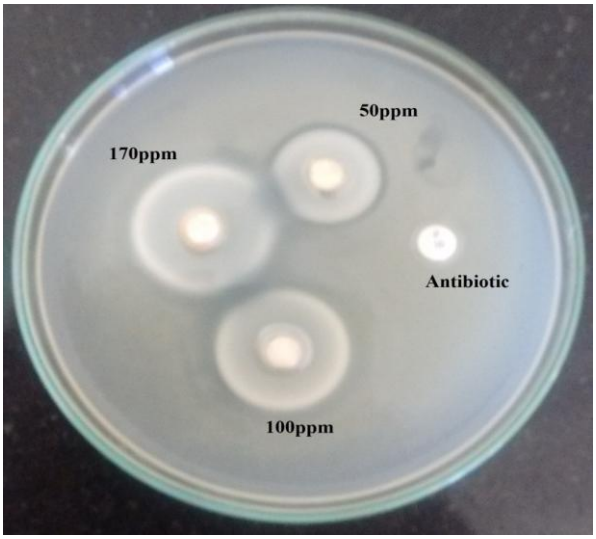

Staphylococcus aureus

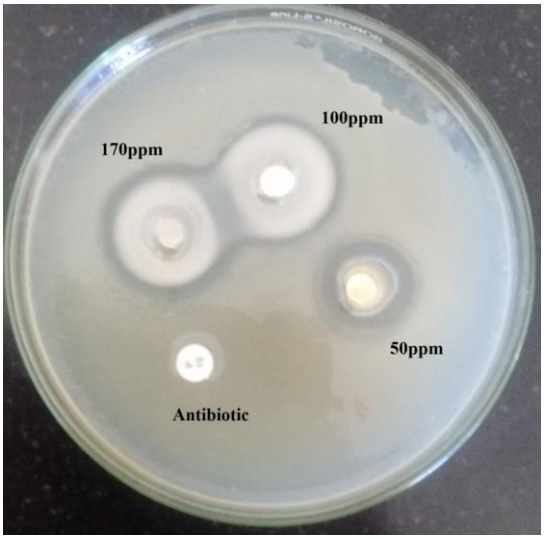

Sphingobacterium thalpophilum

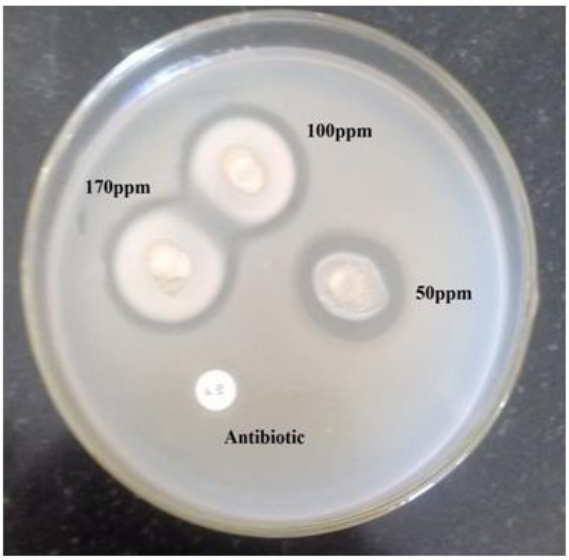

Legionella pneumonia

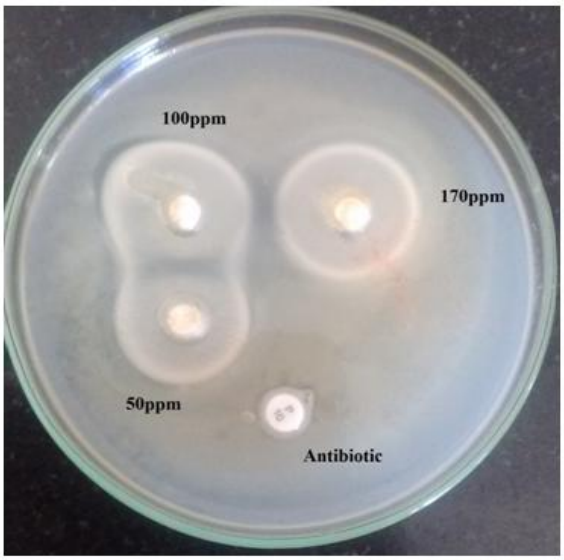

Actinomyces israelii

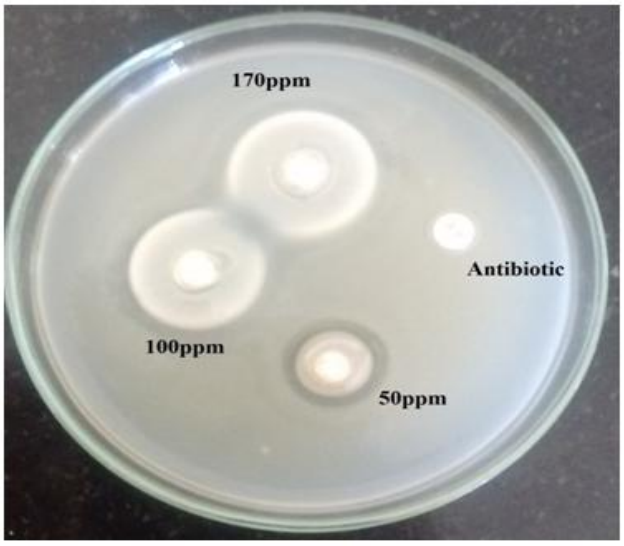

Enterobacter cloacae

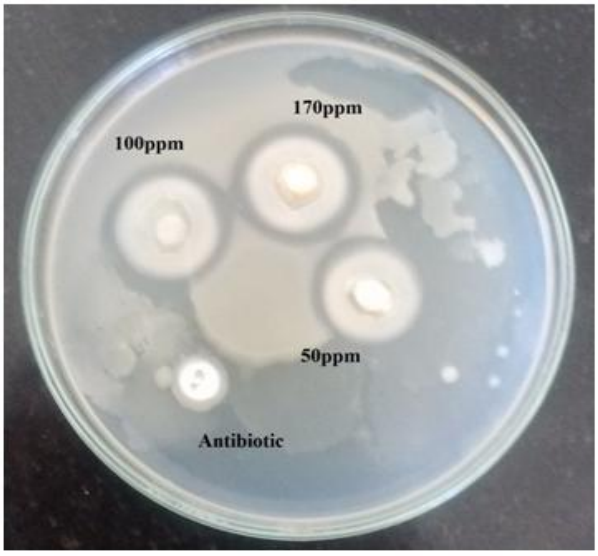

Helicobacter pylori

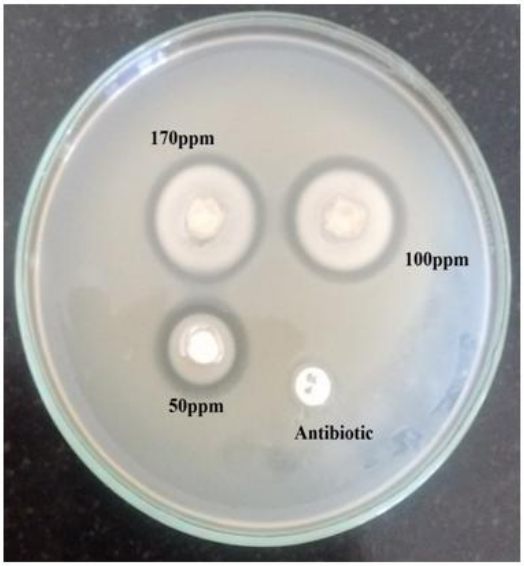

Acinetobacter

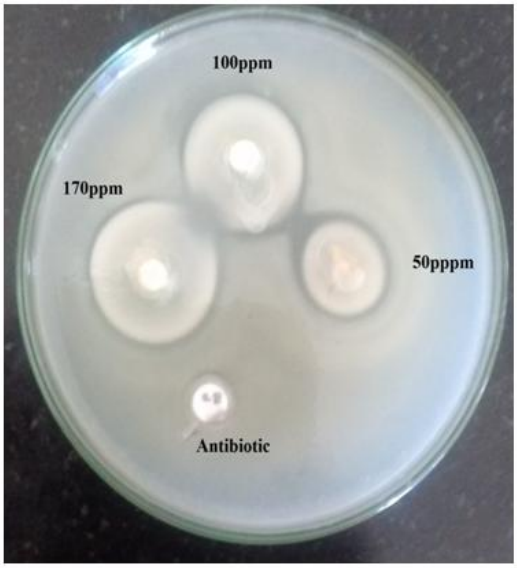

Bacillus subtilis

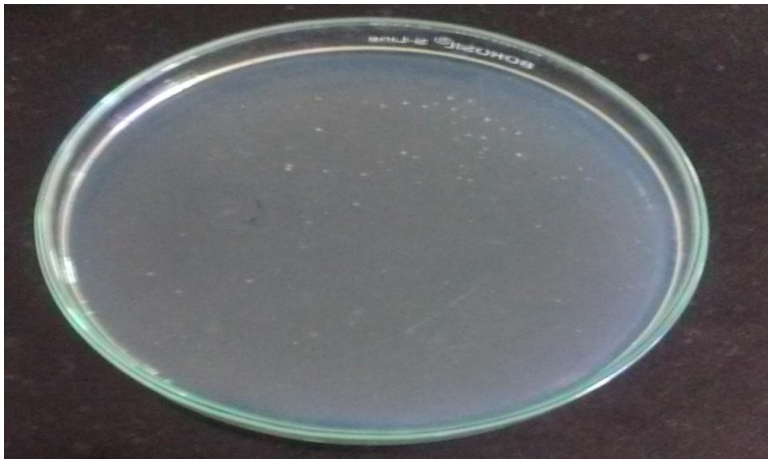

Control

Fig 7a: Showing antibacterial activity of *Sargassum muticum* mediated synthesis of silver nanoparticles

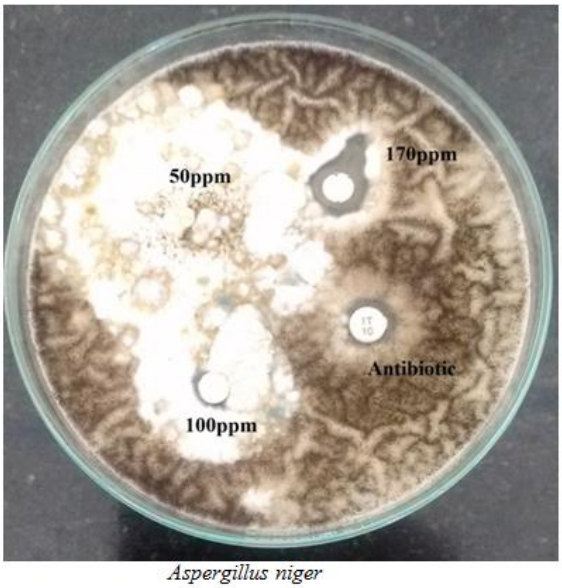

Aspergillus niger

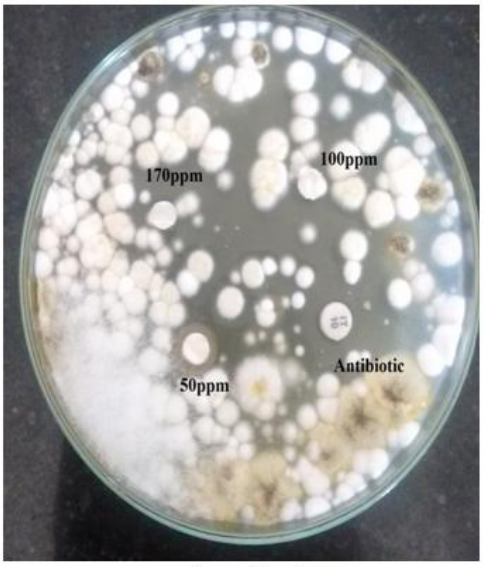

Aspergillus flavus

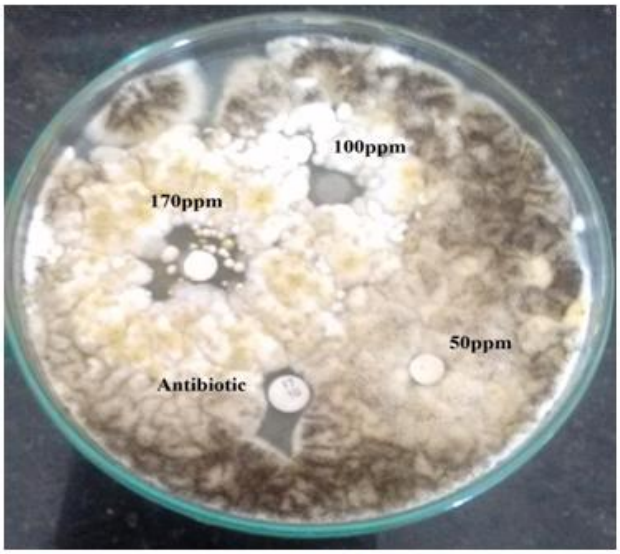

Schelorosium rolfsii

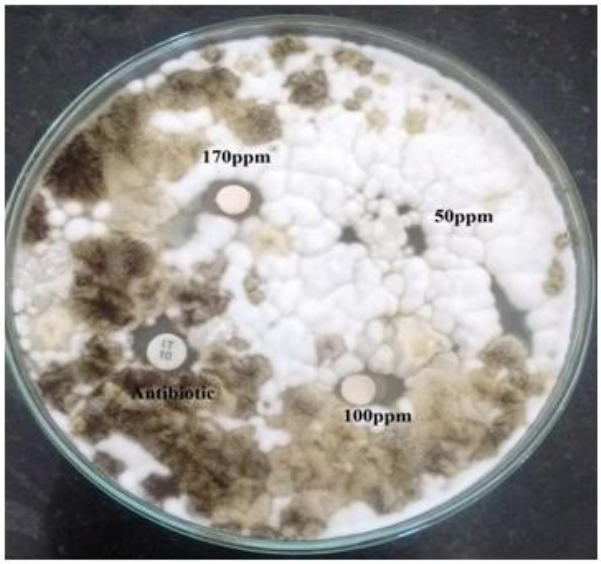

Rhizopus oligosporus

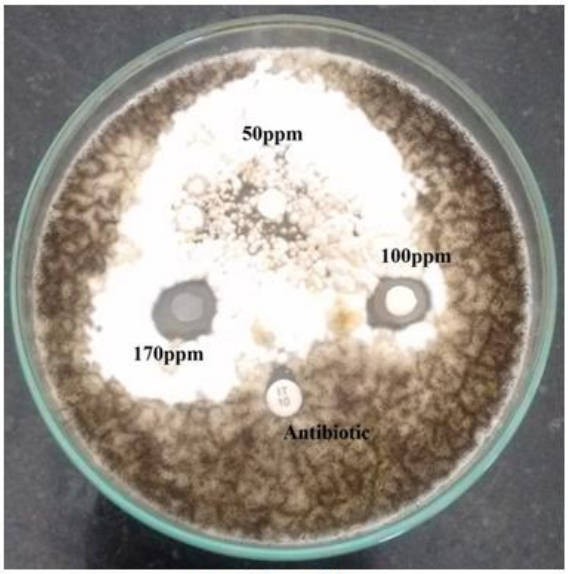

Aspergillus acidus

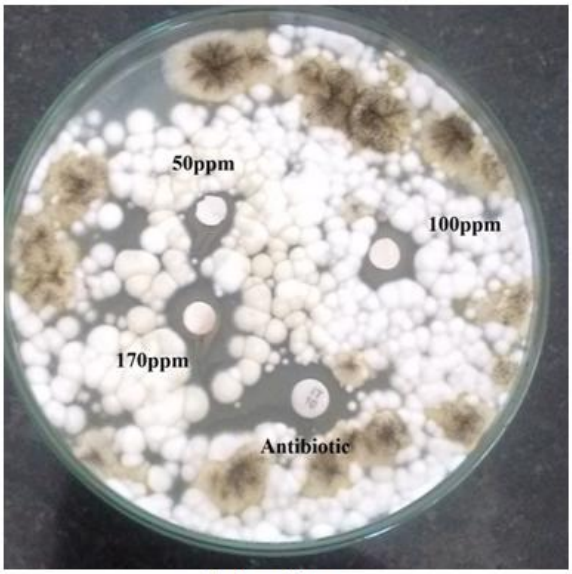

Athelia rolfsii

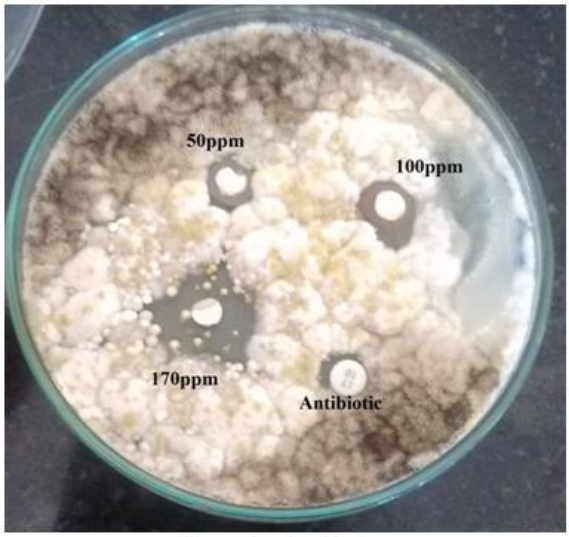

Aspergillus fumigates

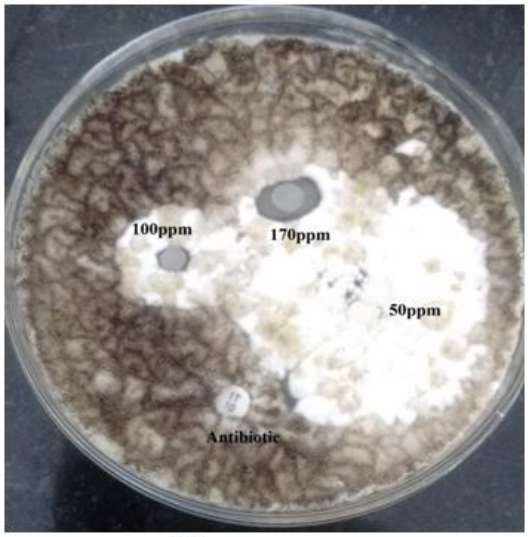

Rhizopus oryzae

Tricoderma asperellum

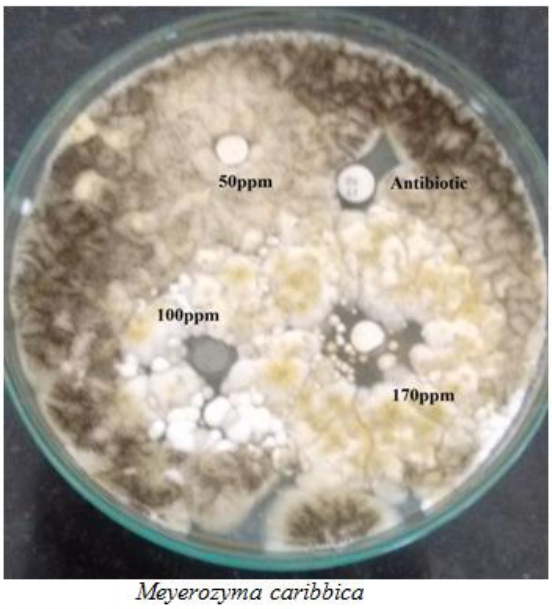

Meyerozyma caribbica

Control

Fig 7b: Showing antifungal activity of *Sargassum muticum* mediated synthesis of silver nanoparticles

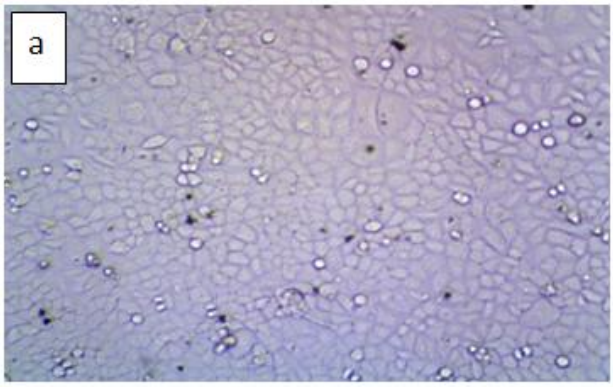

12.5µg/ml

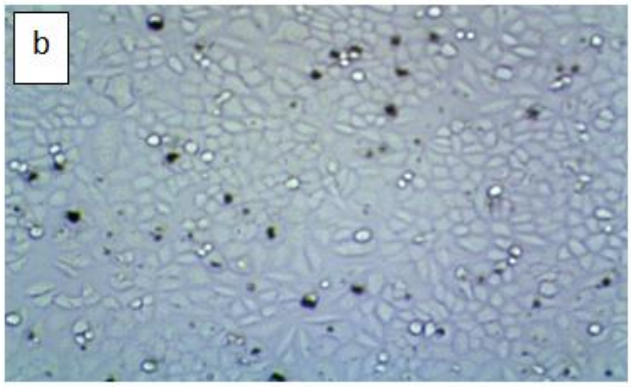

25µg/ml

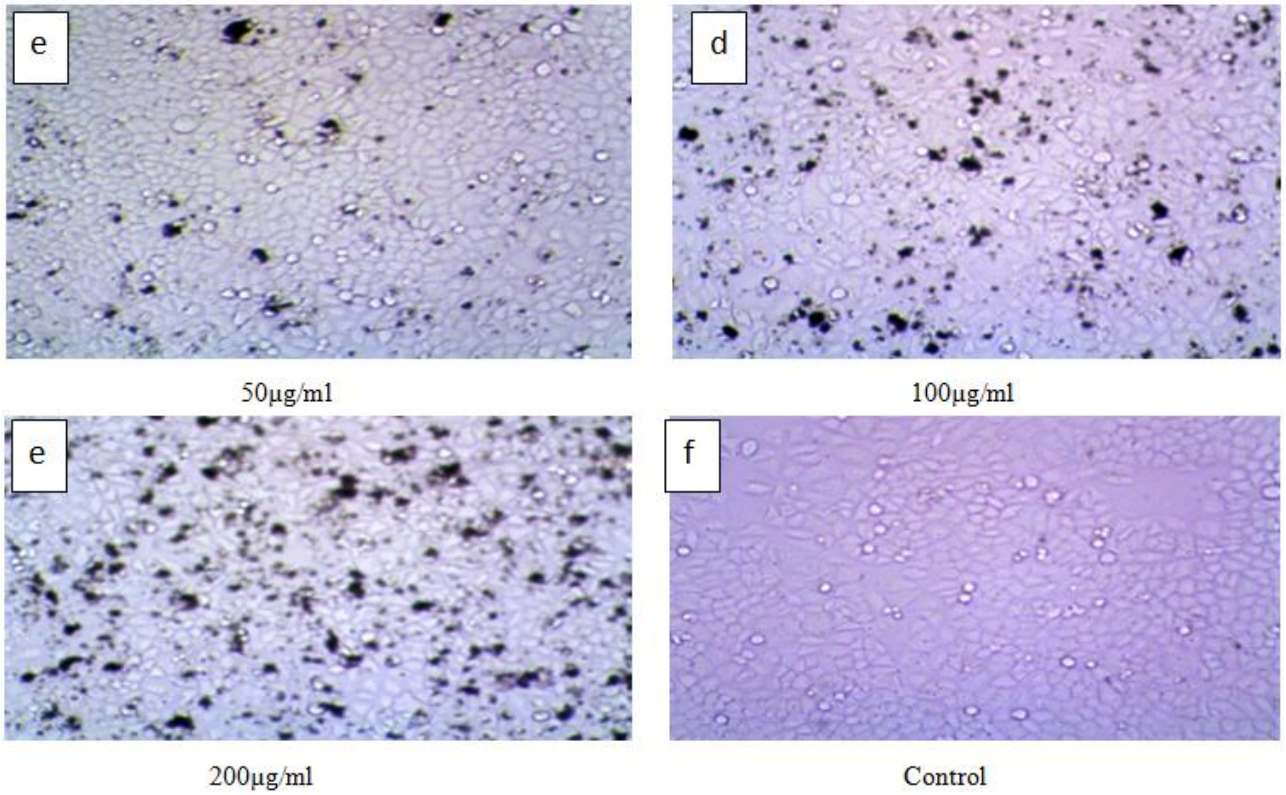

Fig 8: Human Cervical cancer cell line (HeLa) treated with 12.5-200µg/ml of synthesized AgNPs using *Sargassum muticum* aqueous extract

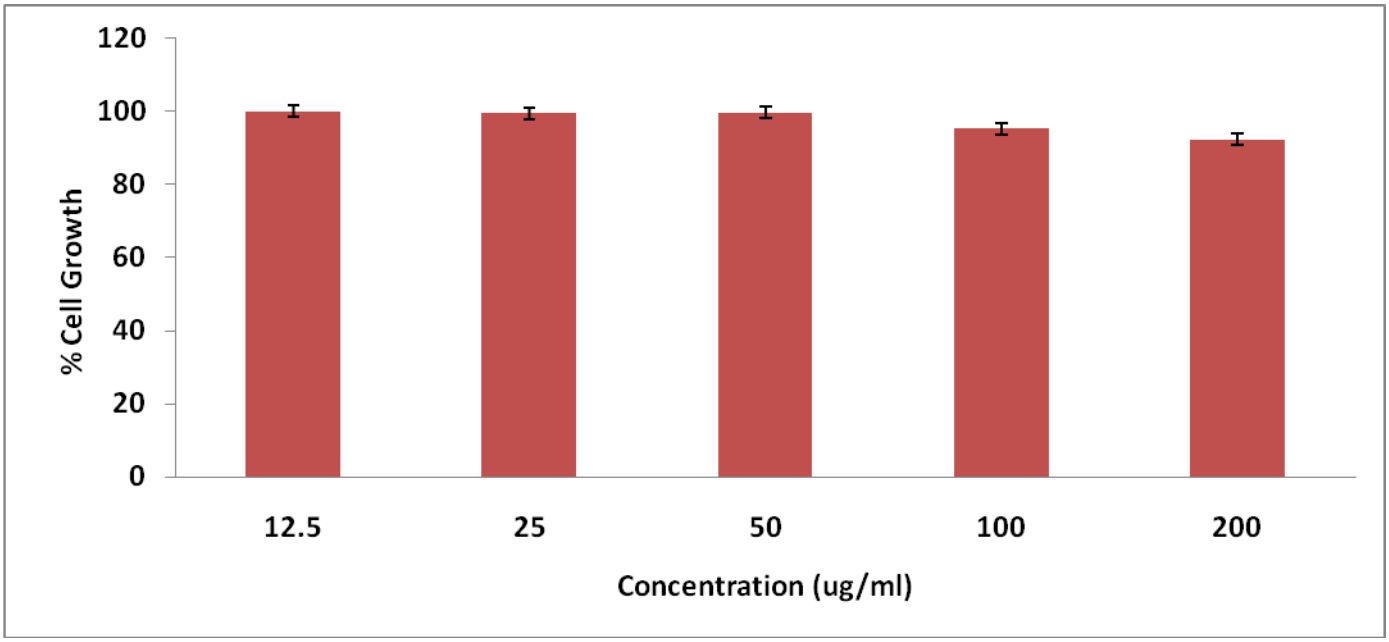

Fig 9: Cytotoxic activity of *Sargassum muticum* AgNPs against Human Cervical cancer cell line (HeLa)

Table I: *In-vitro* antibacterial studies using *Sargassum muticum* mediated synthesis of silver nanoparticles

S.No.	Name of Bacteria	170±ppm	100±ppm	50±ppm	Cefmetazole (30mcg)
1	*E. coli*	2.9±0.12	2.2±0.10	1.8±0.07	1.0
2	*Pseudomonas Fluorescence*	3.0±0.13	2.6±0.10	1.2±0.04	1.0
3	*Staphylococcus aureus*	2.8±0.11	2.5±0.09	1.6±0.06	1.0
4	*Sphingobacterium thalpophilum*	3.0±0.13	2.8±0.08	1.7±0.07	0.8
5	*Legionella pneumonia*	2.7±0.10	2.3±0.06	1.6±0.06	0.6
6	*Actinomyces israelii*	2.9±0.09	2.6±0.07	1.8±0.08	1.0
7	*Enterobacter cloacae*	3.1±0.13	2.0±0.11	1.9±0.09	0.9
8	*Helicobacter pylori*	3.0±0.12	2.5±0.10	1.9±0.09	1.1
9	*Acinetobacter*	3.0±0.12	2.9±0.11	2.6±0.11	1.2
10	*Bacillus subtilis*	2.9±0.09	2.7±0.08	1.6±0.05	1.8

Each value is the ±SE of three measurements

Table II: *In-vitro* antifungal studies using *Sargassum muticum* mediated synthesis of silver nanoparticles

S.No.	Name of Fungus	170±ppm	100±ppm	50±ppm	Itraconazole (30mcg)
1	*Aspergillus niger*	1.9±0.07	1.5±0.05	1.0±0.04	0.4
2	*Aspergillus flavus*	2.1±0.11	1.8±0.09	0.5±0.08	0.6
3	*Schelorosium rolfsii*	1.5±0.06	1.1±0.05	0.5±0.04	0.4
4	*Rhizopus oligosporus*	2.5±0.13	2.0±0.10	1.5±0.07	0.8
5	*Aspergillus acidus*	1.5±0.06	1.0±0.05	0.8±0.03	0.7
6	*Athelia rolfsii*	2.2±0.12	1.8±0.07	0.6±0.05	0.5
7	*Aspergillus fumigates*	2.0±0.10	1.6±0.06	0.8±0.05	1.0
8	*Rhizopus oryzae*	2.2±0.12	1.9±0.08	1.0±0.060.04	0.6
9	*Tricoderma asperellum*	1.5±0.06	1.0±0.05	0.6±0.03	0.8
10	*Meyerozyma caribbica*	2.0±0.10	1.5±0.07	0.6±0.06	1.0

Each value is the ±SE of three measurements

Table III: Cytotoxic activity of *Sargassum muticum* AgNPs against Human Cervical cancer cell line (HeLa)

Conc (µg/ml)	% Cell viability
12.5	100.1138
25	99.4880
50	99.7155
100	95.2787
200	92.2639